Short Paper

A NUMERICAL STUDY OF PILED RAFT FOUNDATIONS

Der-Guey Lin and Zheng-Yi Feng*

ABSTRACT

This paper presents raft-pile-soil interaction for a vertically loaded flexible piled raft on layered subsoil using a two-dimensional finite difference numerical tool. The subsoil is modeled as a linear elastic material and the raft is modeled as a beam structure under plane strain. In addition, the piles are simulated by a series of pile elements considering the pile/soil interface behavior. In the simulations, the required input parameters of soil, pile and interface are determined by back analyses of pile loading tests. Settlement, bending moment, both in pile and raft, as well as effects of raft flexibility for vertical uniform loading in the subsoil were examined. It is found that even though for vertical uniform loading, a relatively high bending moment may be induced in the piles due to lateral displacement of the stressed subsoil. For the case of a piled raft placed over a soft clay layer at ground surface the contact pressure at the raft-soil interface is merely 4 ~ 6% of that developed in the unpiled raft. Nevertheless, the contact pressure may reach 15 ~ 25% of that of the unpiled raft if the piled raft is resting on a sand layer at the ground surface. This implies that the loading carried by the pile group could be reduced by almost 1/4 of the design load and it could eventually reduce the cost of pile group construction to a certain extent.

Key Words: pile, raft, numerical analysis (CI5).

I. INTRODUCTION

Previous studies of Bangkok subsoil had focused mostly on the behavior and performance of single piles. The study of pile groups mostly focused on pile capacity and group settlement without considering the presence of the raft. This fact indicates the necessity of the analysis of a piled raft foundation in Bangkok subsoil.

This study introduces a simple numerical procedure using in-hand finite difference code for piled raft analysis with sufficient accuracy. The piled raft system, at ground level, was assessed and the pile/raft connection was assumed fixed. From the analysis results, readers can obtain ready-made estimation curves for a similar piled raft foundation design in practice. The comparatively high bending moment in vertically loaded piles is noted. In addition, the load carry ratio between raft and piles is investigated for the possible configuration of a piled raft foundation from the stand point of economical design.

*Corresponding author. (Tel: 886-4-22840381 ext. 222; Fax: 886-4-22876851; Email: tonyfeng@dragon.nchu.edu.tw)

The authors are with the Department of Soil and Water Conservation, National Chung-Hsing University, Taichung 402, Taiwan.

II. NUMERICAL MODELING OF PILE LOADING TESTS AND PILED RAFT FOUNDATION

1. Finite Difference Model

The geotechnical finite difference code, FLAC (FLAC, 2002), was applied for this study. For piled raft foundation the soil and structure were discretized into soil element and structural element respectively as shown in Fig. 1. The soil element size close to piles is 1 m × 3 m for stress concentration zone and 3 m × 3 m for soil elements away from piles. To avoid boundary effects the mesh should extend sufficiently beyond the region of interest and eventually the soil mass 90 m × 90 m was discretized into 1,260 rectangular plane strain elements. The adopted domain size

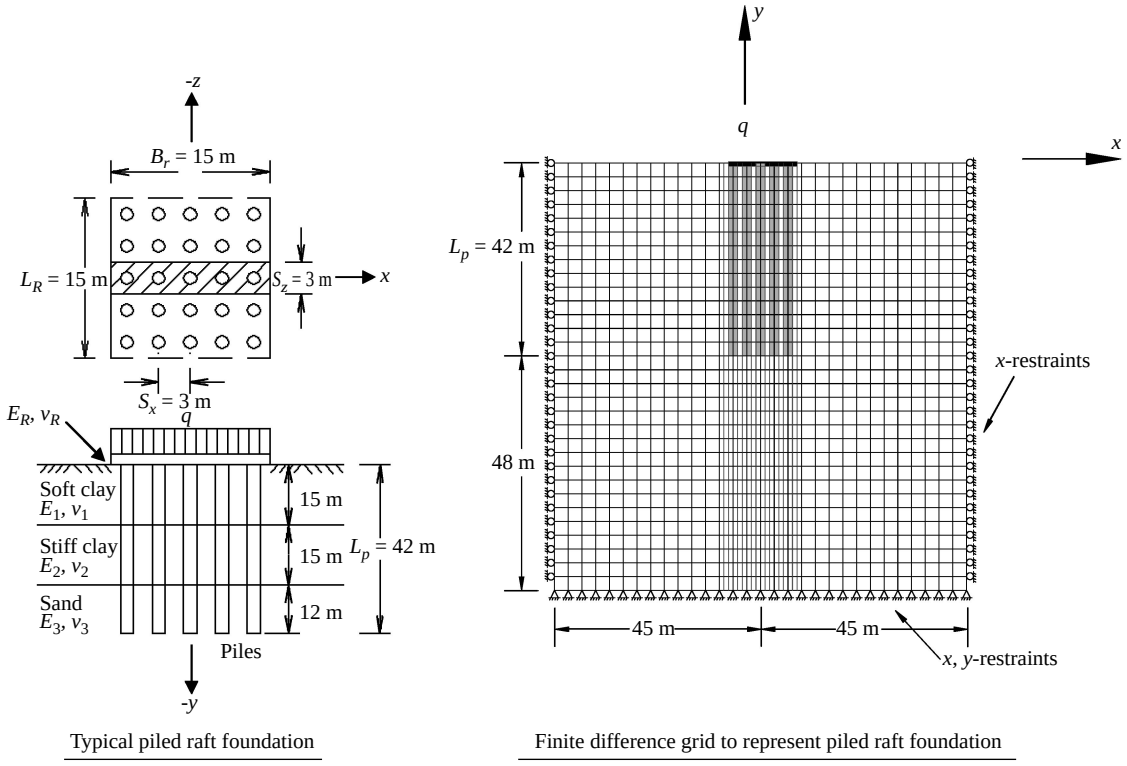

Fig. 1 Typical finite difference discretization of piled raft system

was judged to be sufficient to represent the soil body in the numerical problem by detecting the convergence of numerical solutions for various geometric boundaries. The piles were discretized into 14 pile elements while the raft was discretized into 20 beam elements. The boundary between the raft grid and the soil grid was modeled as an interface and discretized into 20 interface elements. Similar finite difference models were separately prepared for other cases of the piled raft foundation.

2. Structural Elements and Conversion of 3-D Problem to 2-D Plane Strain Model

The beam elements of linear elastic behavior with two nodes and three degree of freedom at each node are used to represent the raft structures where bending resistance is important. The pile elements are adopted to represent the behavior of the piles. The formulation for flexural behavior of the beam elements and pile elements can be found in the documentation of the FLAC program (FLAC, 2002). The pile element interacts with the surrounding soil through coupling springs at the pile/soil interface.

Converting 3-D problems of regularly spaced piles into 2-D plane strain models involves averaging the effect of actual 3-D structures over the spacing in the out-of plane direction. Donovan *et al.* (1984) suggested that linear scaling of material properties is a simple but accurate enough way of distributing the discrete effect of elements over the spacing in a regularly spaced pattern. Therefore, the spacing of piles along the out-of-plane direction, *s*, is used to scale the properties of pile elements. The scaled property is found by dividing the actual property by *s*. Conversely, the actual properties of elements after analysis, such as bending moment and forces, are obtained by multiplying the scaled values by *s*. The strength and stiffness properties of the pile elements and pile/soil interfaces were scaled with spacing, *s*, in the out-of plane direction. The Young's modulus of piles used in this study is $E_c = 2.77 \times 10^4$ *MPa*. Therefore, E_c is scaled by s (3 m pile spacing) into 9.23×10^3 *MPa* for actual input for Young's modulus of the piles.

3. Loading Condition and Configuration of Piled Raft Foundation

The loading was chosen as being in the working range as encountered in Bangkok expressway construction and buildings and a typical vertical uniform working load, *q*, of 333 (kN/m^2) was applied on the piled raft. The thickness of the raft was varied to investigate the effect of the relative stiffness of the raft on load transfer, load carry proportion and settlement of piled raft.

Table 1 Soil properties for numerical model

Soil type	Depth (m)	Unit weight (kN/m^3)	v_s	Estimated S_u (kPa)	Estimated SPT-N	Es (MPa)
Soft clay	0 ~ 15	16.4	0.45	33	–	16.5
Stiff clay	15 ~ 30	20.0	0.35	50	–	60
Silty sand	30 ~ 60	21.0	0.30	–	34	205

Accordingly, piled rafts with different thicknesses (t_R = 0.2 m, 1m and 5 m) and dimensions (width × length = $B_R \times L_R$ = 15 m × 15 m and 30 m × 30 m) were investigated. Checks were also made on the piled raft foundation with regularly spaced piles and typical piled raft configurations for analysis. Results are illustrated in Fig. 2. For pile spacing of 3m the pile configurations in piled rafts are 5 × 5, and 10 × 10 and the corresponding raft dimensions $B_R \times L_R$ are 15 m × 15 m, and 30 m × 30 m. The connection between piles and raft is considered as rigid. The diameter of piles is 1.2 m and the length of piles is 42 m.

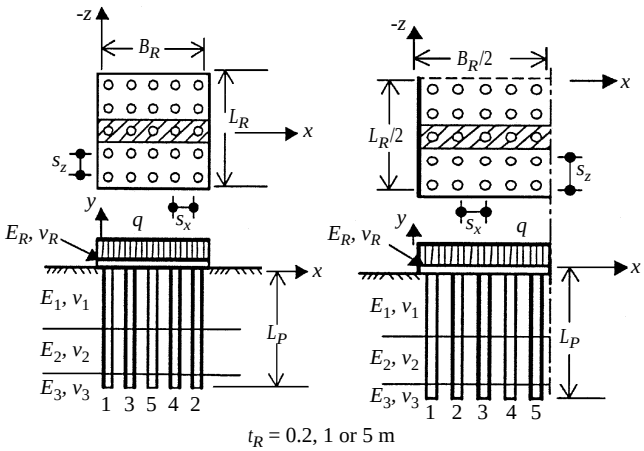

Fig. 2 Typical piled raft configurations for numerical analysis

4. Soil Property and Material Model

The elastic modulus of three layers of Bangkok subsoil, E_s, was estimated by undrained shear strength, S_u, using $E_s = 500 \times S_u$ for the soft clay layer and $E_s = 1{,}200 \times S_u$ for the stiff clay layer while the elastic modulus of the silty sand layer was determined by *SPT-N* value using $E_s = 6{,}000 \times N$ (kPa). On the other hand, the elastic modulus for the piled raft foundation, E_p, was calculated by $E_s = 15{,}000\ (f_c')^{1/2}$ (kg/cm^2) in which the compressive strength of concrete, f_c' is equal to 350 (kg/cm^2). In this study, Poisson's ratio, v_s, of Bangkok subsoil was obtained from previous studies and experiments performed by the Asian Institute of Technology and the subsoil was generalized into three layers for the numerical modeling of pile loading tests and piled raft foundations. The layering generalization adopted is similar to those of Honjo *et al*. (1993). The three layers are predominantly classified into a soft clay layer of depth from 0 ~ 15 m, a stiff clay of depth from 15 ~ 30 m and silty sand for the remaining depth of 30 ~ 60 m. It should be noted that the generalization of subsoils into three layers is not strictly accurate but it may fairly represent the average condition of Bangkok subsoil. The soil properties of the typical Bangkok subsoil are summarized in Table 1. In the numerical analysis, the soils were assumed to behave as linear elastic entities to properly represent the material behavior of the linear load-settlement curve of a static pile loading test with a small displacement level. Similarly, raft and pile were also simulated as elastic structure materials without plastic yielding.

5. Determination of Input Parameters of Coupling Springs

A single pile loading test was performed at the Bangpa-in Pakret expressway project in Thailand. The observed load-settlement curves and load-transfer curves extracted from the test data were used to calibrate the input parameters of coupling springs in this study.

To obtain the real responses of interface behavior, it is necessary to evaluate from a laboratory test or perform a series of parametric studies. Beer (1985) indicated that for a joint in contact, shear stiffness (K_s) and normal stiffness (K_n) of interfaces are theoretically infinite and in the analysis procedure large finite values have to be used. The values for K_s and K_n should be chosen in such a way that the elastic slip and closing is negligible compared to the displacements of the elements adjacent to the joint.

In this study, the stiffness of coupling springs was initially estimated from the elastic modulus of surrounding subsoil, E_s, for the numerical simulation of a pile loading test. The load transfer curve was used for comparison and finally to obtain the optimum values of shear stiffness, K_s and normal stiffness, K_n. In summary, the values of K_s and K_n for the soil layers in the pile load test site were (0.34 ~ 0.38) × E_s and (1.35 ~ 3.8) × E_s respectively. For interface strength parameters, the cohesive strength parameter C_s and C_n of clay layer

Table 2 Input parameters of pile-soil interface and raft/soil interfaces

Pile/soil interface (Soil type)	K_s (N/m^2)	ϕ_s (°)	c_s (N/m)	K_n (N/m^2)	ϕ_n (°)	c_n (N/m)
Soft clay	5.670×10^6	0	1.035×10^5	6.258×10^7	0	2.376×10^5
Stiff clay	2.220×10^7	0	1.749×10^5	9.630×10^7	0	1.290×10^6
Silty sand	7.884×10^7	21	0	2.760×10^8	21	0
Raft/soil interface (Soil type)	K_s (N/m^2)	ϕ_s (°)	c_s (N/m)	K_n (N/m^2)	ϕ_n (°)	c_n (N/m)
Soft clay	5.670×10^6	0	1.035×10^5	6.258×10^7	0	2.376×10^5

and frictional strength parameter ϕ_s and ϕ_n of sand layer of interface were estimated from the strength parameters c and ϕ of surrounding subsoil. The interface cohesive strength parameters for the sand layer and the interface frictional strength parameters for clay layers were ignored. The required input parameters of pile/soil interface obtained from back analysis of the single pile loading test are summarized in Table 2. Note that the actual input parameters of pile/soil interface for K_s, K_n, C_s, and C_n should also be scaled by the pile spacing, s, for 2D plane strain analysis to simulate regularly spaced structural elements (FLAC, 2002).

III. NUMERICAL RESULTS OF PILED RAFT FOUNDATION

The responses of piled raft foundations of different configurations (supported by 5 ×5 piles with $B_R \times L_R$ = 15 m ×15 m and 10 ×10 piles with $B_R \times L_R$ = 30 m ×30 m) located at the ground level were investigated under a uniform vertical loading of q = 333 kPa.

1. Effect of Raft Stiffness on Settlement

The settlement of the piled rafts of different dimensions ($B_R \times L_R$ = 15 m ×15 m and 30 m ×30 m) is shown in Fig. 3(a) and (b). Note that vertical settlements are denoted by negative values in this study for consistency with the numerical output. The induced settlement of the piled raft was expressed in terms of normalized distance, x/B_R, as an abscissa and normalized settlement, $I = w_i E_s / qB_R(1 - \nu_s^2)$, as an ordinate in which w_i is settlement at point i, E_s is the Young's modulus of soft clay, ν_s is the Poisson's ratio of the soft clay layer, q is the uniformly distributed vertical loading at raft surface. As shown in Fig. 3(a) and (b), the thickness of the piled raft merely displays a minor effect on the normalized settlement in the case of the smaller raft dimensions of 15 m × 15 m (5 × 5 piles). On the other hand, the differential settlement of a thin piled raft (t_R = 1 m) appears more prominent than that of a thick piled raft (t_R = 5 m) in the case of larger

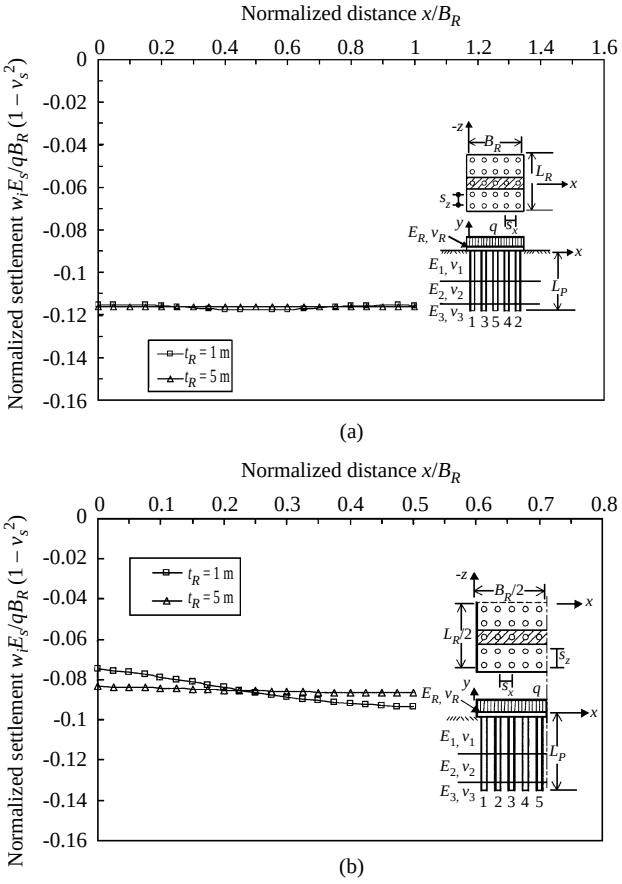

Fig. 3 (a) Normalized settlement of piled raft with $B_R \times L_R$ = 15 m × 15 m (5 × 5 piles) or different raft thicknesses, raft edge-to-raft edge plot. (b) Normalized settlement of piled raft with dimensions $B_R \times L_R$ = 30 m × 30 m (10 × 10 piles), raft edge-to-raft center plot.

dimension of 30 m × 30 m (10 × 10 piles) as indicated in Fig. 3(b). Meanwhile, the thin piled raft (10 × 10 piles with $B_R \times L_R$ = 30 m × 30 m) frequently shows a bowl-shaped settlement pattern at the piled area and larger differential settlement than the thick piled raft. It can be seen that the normalized settlement of the thin piled raft varies from -0.074 (w_i = 36.0 mm) at the raft edge to -0.093 (w_i = 45.2 mm) at raft center while the

thick piled raft shows almost identical values of normalized settlement from -0.083 (w_i = 40.3 mm) at the raft edge to -0.087(w_i = 41.9 mm) at the raft center. The thin piled rafts exhibit less settlement than thick piled rafts near the edge area for a $x/B_R < 0.225$.

The effect of the raft stiffness is depicted in the Figs. 4(a) and (b) with relative raft stiffness, $K_R = 4E_R(1 - \nu_s^2)t_R^3/3E_s(1 - \nu_R^2)B_R^3$ and normalized settlement, similar to the plots of Ta and Small (1997). The symbols E_R, ν_R and t_R represent the Young's modulus, Poisson's ratio and thickness of the raft respectively. It is seen that in Fig. 4(b) the settlement of the edge point (*point 1*) increases as the raft stiffness, K_R, increases. Contrary to the edge point, the inner points (*point 3, 4 and 5*) of the raft show a decreasing trend in settlement as K_R increases. Conclusively, for $K_R > 10$ the magnitudes of settlements along the transverse strip of raft can practically be regarded as on the same level. Similarly, for $K_R < 0.01$ the settlements of raft points merely display slight variations with changing K_R value whereas the settlements of the edge and inner points are distinctly different in magnitude. The region $0.01 < K_R < 10$ can be regarded as a transitional zone where the raft settlement exhibits sensitivity to the relative raft stiffness. This zone is also a matter of practical concern because most rafts lie in this range. For most reinforced concrete rafts in practice, the relative raft stiffness K_R falls in the range $0.01 < K_R < 10$ and hence, it has implications on the practical design of the raft.

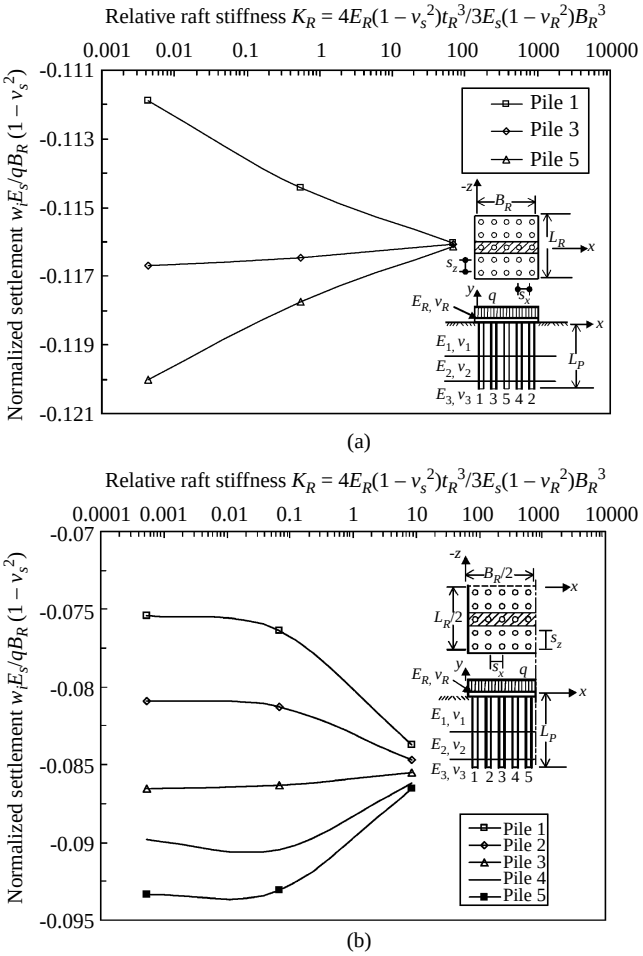

Fig. 4 (a) Effect of raft stiffness on settlement of piled raft with dimension $B_R \times L_R$ = 15 m × 15 m (5 × 5 piles), raft edge-to-raft edge plot. (b) Effect of raft stiffness on settlemtn of piled raft with dimension $B_R \times L_R$ = 30 m × 30 m (10 × 10 piles), raft edge-to-raft center plot.

2. Effect of Raft Stiffness on Bending Moment

Plane strain bending moments (M_{PS} in kN-m/m) of the piled rafts were investigated in terms of normalized bending moment ($M_{PS} \times 100/qB_R^2$) and normalized distance (x/B_R) for different raft thicknesses (t_R = 1 m and 5 m) and different raft dimensions ($B_R \times L_R$ = 15 m × 15 m and 30 m × 30 m). As illustrated in Figs. 5(a) and (b), the bending moment of the piled raft was investigated for a surface piled raft (supported by 5 × 5 and 10 × 10 piles at ground surface). It was observed that for all types of configuration the bending moment of a thick piled raft (t_R = 5 m) is higher than that of a thin piled raft (t_R = 1 m) and a larger raft ($B_R \times L_R$ =30 m × 30 m) displays much higher bending moment than a smaller raft ($B_R \times L_R$ =15 m × 15 m).

The bending moments of the piled rafts show sharp turnings at the pile points and it was shown that the bending moments sag at the pile points and peak at raft spans. The calculated bending moments are also compared with those of Ta and Small (1997) with fair agreement. The slight difference might be due to the differences in the degree of discretization and modeling discrepancies. The present analysis models the raft as a beam strip while Ta and Small (1997) considered it as a plate structure.

The thick piled raft (t_R = 5 m) induces higher normalized bending moment of 2.08 (or M_{PS} = 6233.8 kN-m/m) than the 0.218 (M_{PS} = 653.3 kN-m/m) of the thin piled raft (t_R = 1 m) for a raft dimension $B_R \times L_R$ = 30 m × 30 m supported by 10 × 10 piles.

3. Contact Pressure at Piled Raft/Soil Interface

The contact pressures at raft/soil interface were investigated for a piled raft with dimensions $B_R \times L_R$ =15 m × 15 m supported by 5 × 5 piles at ground surface under vertical uniform loading as shown in Fig. 6. The load transferred from the raft to soil is calculated from the contact pressure, σ_v, induced at the raft/soil interface. An un-piled raft test is performed for comparison purposes. It is shown that the contact pressure of the piled raft is lower than that of the unpiled raft and is merely 4 ~ 6% of that developed in the unpiled rafts resting on the soft clay layer.

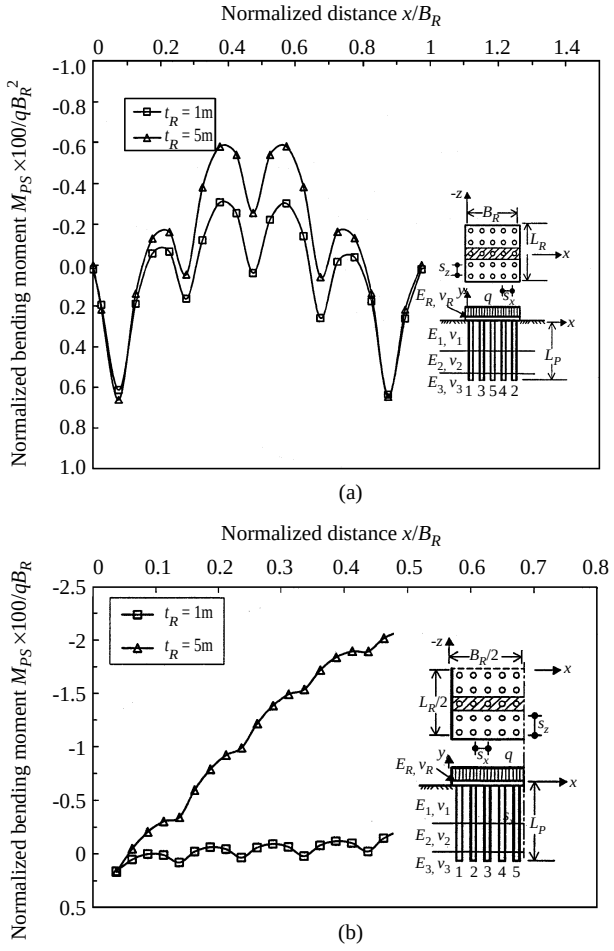

Fig. 5 (a) Bedning moment of piled raft with dimensions $B_R \times L_R$ = 15 m × 15 m (5 × 5 piles), raft edge-to-raft edge plot. (b) Bending moment in piled raft with dimensions $B_R \times L_R$ = 30 m × 30 m (10 × 10 piles), raft edge-to-raft center plot.

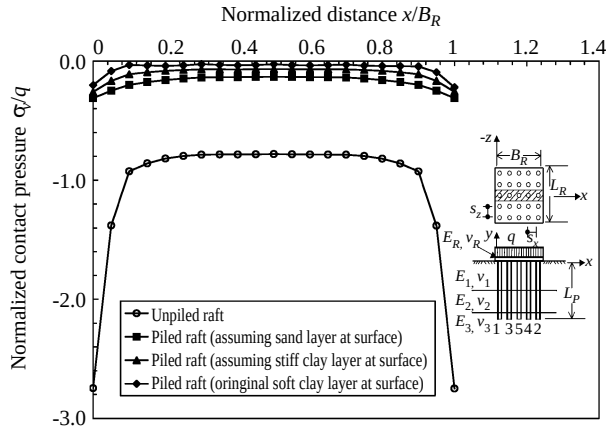

Fig. 6 Comparison of contact pressure at raft-soil interface among piled rafts and unpiled raft, t_R = 1 m, raft edge-to-raft edge plot

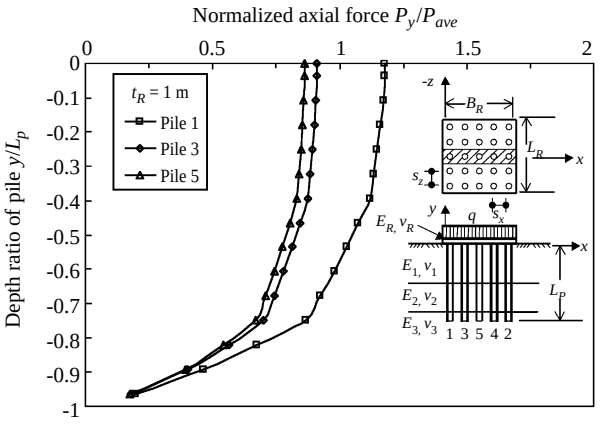

Fig. 7 (a) Axial force distribution in pile structure of piled raft with diemensions $B_R \times L_R$ = 15 m × 15 m (5 × 5 piles), L_p = 42 m, q = 333 kPa.

This is due to the fact that a high proportion of the loading is transferred directly through the piles to the underneath bearing zone.

To further investigate the influence of soil stiffness on contact pressure issues, the stiff clay and silty sand layers of Bangkok subsoil are fictitiously assumed as surface layers for two additional analyses. The two additional contact pressure results are also plotted in Fig. 6. For a piled raft resting on the stiff clay at ground surface, the contact pressure is increasing to 7 ~ 10% of that developed in the unpiled rafts resting on the soft clay layer. Moreover, for a piled raft resting on the sand layer at ground surface, the contact pressure is further increasing to 15 ~ 25% of that developed in the unpiled rafts. This implies that the loading carried by the pile group could be reduced by almost 1/4 of the design loading. Consequently, one-fourth of the cost of pile construction can be saved if the surface layer of soil stratum is a stiffer silty sand layer rather than a soft clay layer. From numerical results, it is indicated that the contact pressure and load carrying ratio of a piled raft are similar in both cases of raft thickness of t_R = 5 m and t_R = 1.0 m. Eventually, a summary conclusion can be made that the piled raft is capable of carrying more loading and reducing the loading burden on the pile group to a certain extent, if the soil layer beneath the piled raft possesses sufficient stiffness. Nevertheless, the settlement of the piled raft should be carefully examined if the compressibility of soil layers appears significant.

4. Axial Force in Piles

The axial forces of a pile in a pile group were calculated for a surface piled raft supported by 5 ×5 piles at ground surface under vertical uniform loading as shown in Fig. 7. The piled raft possesses dimensions of $B_R \times L_R$ =15 m ×15 m and a thickness of t_R = 1 m. It is indicated that the outermost piles (*pile-1*) in the pile group take higher axial loads than the inner

piles (*pile-3* and *pile-5*). The maximum normalized axial load carried by outermost piles can reach 1.25 $\times P_{ave}$ while it becomes 0.8 $\times P_{ave}$ at the inner piles. In which, the P_{ave} value is an average loading defined by the total vertical load divided by the number of piles. This highlights the importance of the proper design of the outermost piles in the piled raft system.

5. Bending Moment in Piles

As shown in Fig. 8, for vertical uniform loading, as the pile group possesses a rigid connection with a thin raft (t_R = 1 m), the pile shaft at the elevations of pile/raft connection points, at the middle depth of the soft clay layer and at the transitions of soil layers may all induce relatively high bending moments (M_{PL} in kN-m/m). This implies heavy reinforcements should be considered at the aforementioned pile elevations in structural design of the piled raft. It is worthwhile to emphasize again that even though the loading is vertical, it produces large bending moments in the piles due to lateral displacement of the stressed subsoil. The phenomenon is often neglected in design practice and may lead to unsafe design.

IV. CONCLUSIONS

In this paper two-dimensional finite difference method with plane strain condition was applied to study pile-raft-soil interaction in layered Bangkok subsoil.

The analysis indicates that thick rafts induce higher bending moments than thin rafts. Meanwhile, the relative raft stiffness K_R in the region $0.01 < K_R < 10$ (1 m < t_R < 5 m) can be regarded as a transitional zone where the raft settlement exhibits high sensitivity to the raft thickness. This zone is also a matter of practical concern because most of the reinforced concrete piled rafts lie in this range.

The normalized bending moment of a piled raft is generally lower than that of an unpiled raft. Similar to the unpiled raft, the thick piled raft (t_R = 5 m) induces higher bending moment than the thin piled raft (t_R = 1 m) for the case of raft dimension $B_R \times L_R$ =30 m ×30 m supported by 10 ×10 piles.

The maximum normalized axial load carried by outermost piles can reach 1.25 $\times P_{ave}$ while it is becomes 0.8 $\times P_{ave}$ at the inner piles for t_R = 1 m. The induced maximum axial forces on a pile highlight the importance of the proper design of the outermost piles in the piled raft system.

For vertical uniform loading, relatively high bending moment may be induced in the piles due to lateral displacement of the stressed subsoil. Heavier reinforcements are then suggested for installation at those sections with high bending moments.

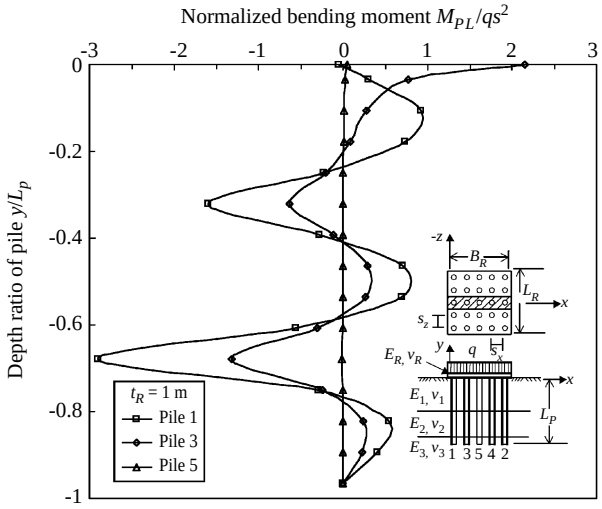

Fig. 8 Bending moment distribution in pile structure of piled raft with dimensions $B_R \times L_R$ = 15 m × 15 m (5 × 5 piles), L_p = 42 m, q = 333 kPa.

The contact pressure developed in the raft-soil interface for a piled raft resting on a soft clay layer surface is insignificant (only 4 ~ 6% of total loadings) and most of the loadings are carried by the piles. For the piled raft constructed over a stiffer soil layer, the contact pressure becomes 15 ~ 25% of the total loading. This implies that the loading carried by the pile group could be reduced by almost 1/4 of the design loading.

REFERENCES

Beer, G., 1985, "An Isoparametric Joint/Interface Element for Finite Element Analysis," *International Journal for Numerical Method in Engineering*, Vol. 21, pp. 585-600.

Donovan, K., Parisuau, W. G., and Cepak, M., 1984, "Finite Element Approach to Cable Bolting in Steeply Dipping VCR Slopes," *Geomechanics Application in Underground Hardrock Mining*, pp. 65-90, Society of Mining Engineers, New York, USA.

FLAC, 2002, Fast Lagrangian Analysis of Continua, *User's Manual*, Version 4.0, Itasca Consulting Group, Inc, Minneapolis, MN, USA.

Honjo, Y., Limanhadi, B., and Liu, W. T., 1993, "Prediction of Single Pile Settlement Based on Inverse Analysis," *Soil and foundations*, Vol. 33, No. 2, pp. 126-144.

Ta, L. D., and Small J. C., 1997, "An Approximate Analysis of Raft and Piled Raft Foundations," *Computer and Geotechnics*, Vol. 20, No. 2, pp. 105-123.

Manuscript Received: Feb. 25, 2005
Revision Received: Sep. 07, 2005
and Accepted: Oct. 03, 2005